Effect of topographical nanopatterning on osteoblastic differentiation

Chang-Su Kim

The Graduate School

Yonsei University

Department of Dentistry

Effect of topographical nanopatterning on osteoblastic differentiation

A Dissertation

Submitted to the Department of Dentistry

at the Graduate School of Yonsei University

in partial fulfillment of the

requirements for the degree of

Doctor of Philosophy of Dentistry

Chang-Su Kim

July 2015

This certifies that the dissertation of
Chang-Su Kim is approved.

Thesis Supervisor: Kee-Joon Lee

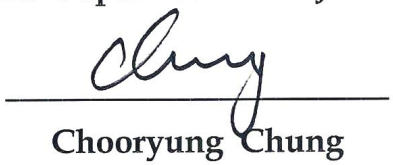

Chooryung Chung

Seok Jun Moon

Hyun Sil Kim

Hang-Rae Kim

The Graduate School of
Yonsei University
July 2015

Table of Contents

Legend of Figures

Legend of TABLEs

ABBREVIATION

Ad-MSC: adipose tissue-derived mesenchymal stem cell

AFM: atomic force microscope

ALP: alkaline phosphatase

ARS: alizarin red staining

CA: contact angle

ERK: extracellular signal-regulated kinase

pERK: phosphorylated extracellular signal-regulated kinase

FAK: focal adhesion kinase

IHC: immunohistochemistry

NF-κB: nuclear factor kappa-light-chain-enhancer of activated B cells

pNF-κB: phosphorylated nuclear factor kappa-light-chain-enhancer of activated B cells

HOPP: 2-hydroxy-2-methyl-propiophenone

PDLSC: periodontal ligament stem cells

PDMS: poly dimethylsiloxane

PIASxβ: Protein Inhibitor of Activated STAT (PIAS), 2

PS: polystyrene

RUNX2: Runt-Related Transcription Factor 2

SEM: scanning electron microscopy

TPT: trimethylolpropane propoxylate triacrylate

UVO: ultraviolet ozone

Abstract

Effect of topographical nanopatterning on osteoblastic differentiation

Surface topographies have been demonstrated to have an effect in various types of cells because living cells can sense the local geometry of extracellular matrix to control their own shape, activation, differentiation, motility, and fate. For instance, the surface modifications of dental implants have an influence on their success by modulating osteoblastic differentiation *in vivo*. Even now, the ongoing studies has been continued to develop the good surface topography that improves bone deposition with an earlier and longer functional implant. However, no one sought the rule of topography to enhance the differentiation of osteoblast.

In this study, various topographical groove patterned trimethylolpropane propoxylate triacrylates (TPT) were made and selected to enhance the differentiation of osteoblast with preosteoblast cells such as murine MC3T3-E1 cells, human adipose tissue derived mesenchymal stem cell, and human periodontal ligament stem cells. Osteoblastic differentiation was evaluated by mineralization using Alizarin red S. staining and the mRNA expression of osteoblastic markers. In addition, a groove pattern was analyzed mechanism by which strengthens the differentiation of osteoblasts.

As results, the differentiation of osteoblasts on the specific groove pattern was

enhanced compared to the nonpattern in terms of differentiation time, the amount of osteogenic factors (about a half dose), or in the condition of a tenth seeding condition (about one tenth number). The ERK phosphorylation and the type I collagen expression of cells on the specific groove pattern were upregulated, suggesting that a tensile stress might affect the differentiation of osteoblast.

Taken together, these results suggest that a specific topographical groove pattern could enhance osteogenesis, even though sub-optimal condition as for nonpattern, through tensile stress and might be good dental and orthopedic materials.

Key words: topographical pattern, osteoblast differentiation, tensile stress

Effect of topographical nanopatterning on osteoblastic differentiation

Chang-Su Kim

The Graduate School Yonsei University

Department of Dentistry

(Directed by prof. Kee-Joon Lee, D.D.S., M.S.D., Ph.D.)

I. Introduction

Osseointegration is a direct bone-to-metal interface without interposition of non-bone tissue. This concept has been described by Branemark; "a direct structural and functional connection between ordered, living bone and the surface of a load-carrying implant" [1] (Figure 1). For instance, osseointegration is critical for the clinical success of dental implants and orthopedic devices. Therefore, various surface patterns of titanium dental implants were made to enhance the osseointegration of titanium dental implants since surface roughness was thought be critical factor (Figure 2). Given that rough-surfaced implants favor both bone anchoring and biomechanical stability, research for surface topography holds great significance for designing biomaterials to enhance osseointegration by the differentiation of osteoblast.

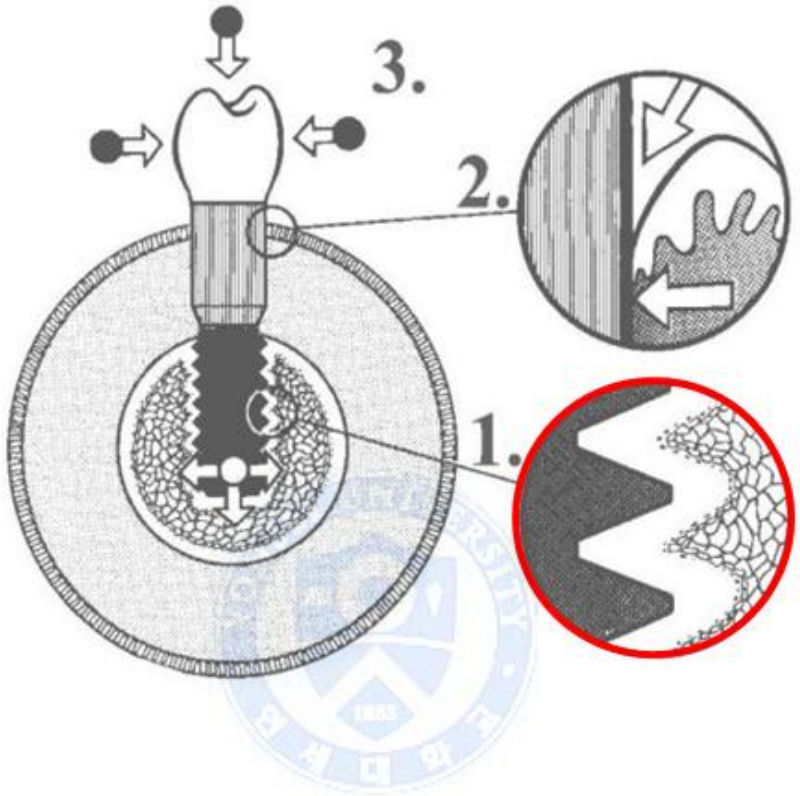

Figure 1. Scheme of biointegration of a dental implant, representing osseointegration (1), mucosal seal (2) and biomechanical forces (3). The success and the long-term prognosis of dental implants depend mainly on three factors: 1) on the anchorage of the artificial root in the host bone, *i.e.* on the osseointegration; 2) on the peri-implant mucosal seal; 3) finally on the adequate loading of the implant, transmitted by the abutment, *i.e.*, the biomechanical factor.

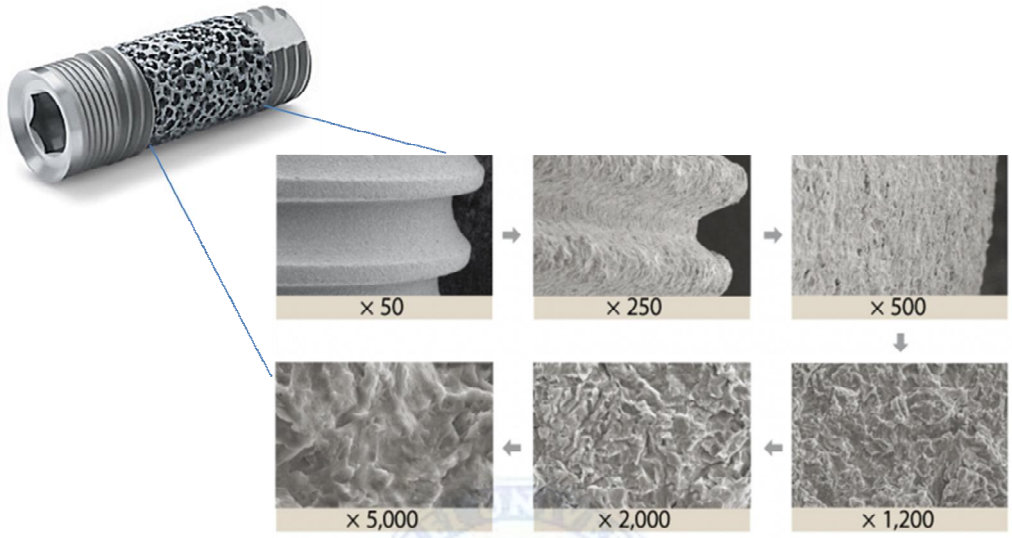

Figure 2. Surface topography on the surface material was irregularly rough. Surface roughness on the fixture was observed by SEM (modified the picture from ZIMMER and OSSTEM). Topography was not smooth but irregular when it was taken pictures at the high magnification.

However, currently there is limited development of surface topography for enhancing osseointegration than expected although considerable amounts of ongoing research have been doing for surface topographies. There are possible reasons. First, the understanding of surface topologies for osteoblastic differentiation and mechanism therein are remained unclear. Second, it is difficult to make the designed or desired surface topographies for evaluating the differentiation of osteoblasts.

It has been known that surface topographies have effects in various mammalian cells [2]. Because living cells can sense the local geometry of complex and well-defined structures (*i.e.*, contact guidance) of extracellular matrix (ECM) to control their own shape, motility, tensile stress [3], and fate [4], such contact guidance describes the phenomenon by which cells recognize and respond to altered extracellular topography by changing their morphology, orientation, and behavior, resulting in altered signaling event such as focal adhesion kinase (FAK). Thus, these extracellular microenvironments play a fundamental role in directing and mediating the differentiation of cells.

Extracellular microenvironment was conveyed into cells through both receptor ligand interactions, as well as mechanical signaling events, which in turn stimulate the important signal transduction pathways and control the cellular function [5]. Among them, the skeletal system developed and adapted by hormones, cytokines, and physical factors such as mechanical stress. The bone mass of adults is maintained by a dynamic process involving a balance of bone remodeling by osteoblasts and osteoclasts [6]. Mechanical stress is known to

influence both bone formation and bone resorption. Importantly, tensile stress promotes bone formation, while the lack of physical stress, as in immobilization, results in disuse osteopenia or osteoporosis. Similarly, orthodontic tooth movement necessitates bone resorption at the pressure side with concomitant bone formation at the tension side. Tensional homeostasis between and within cells contributes to proper cell differentiation, development, and survival eventually [7]. In detail, tensile stress is crucial factor for osteogenesis of human mesenchymal stem cells (MSCs) and osteoblasts. Ikegame *et al.* reported that that tensile stress induced osteoblast differentiation, leading to osteogenesis in mouse calvarial sutures in culture [8]. Tensile stress stimulated the mechano-signal transduction pathways that are involved in the up-regulation of *COL I* gene [9] (Figure 3). With this regard, it has been shown that the mitogen-activated protein kinases (MAPKs) are the most prominent kinase activated by mechanical stress [10, 11].

Thus I have a question which topographical patterns enhance osteoblastic differentiation and what mechanism is involved therein. To address this issue, designed groove patterns were fabricated onto TPT and used for the differentiation of osteoblast with three kinds of different cells. Signaling pathways also were analyzed to prove the mechanism from optimal topographical pattern.

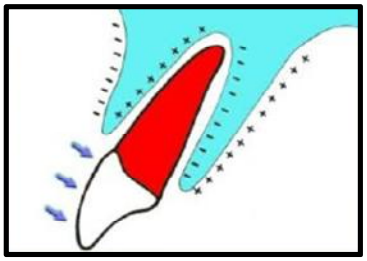

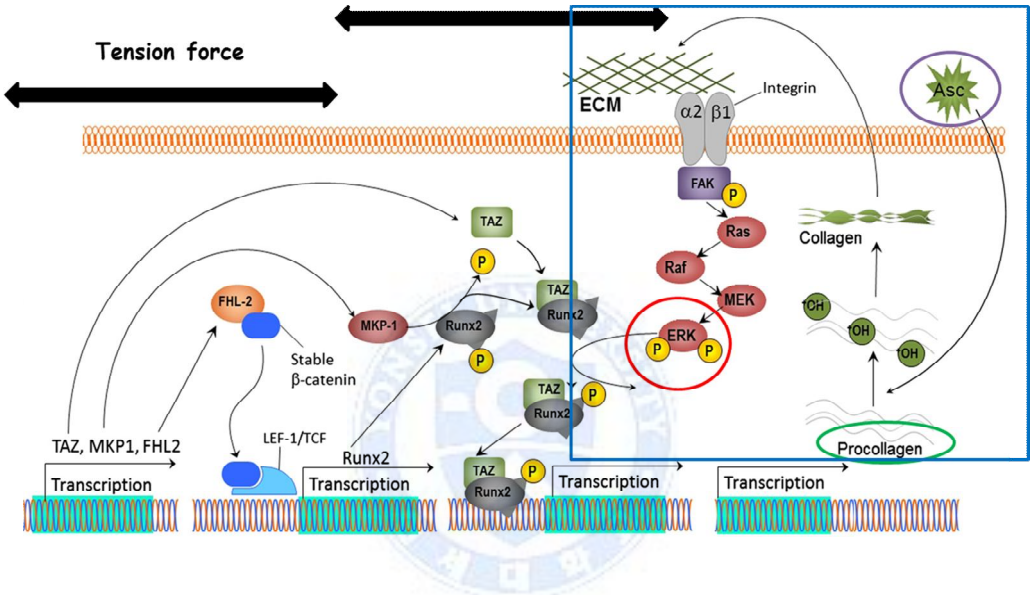

Figure 3. Schematic diagram of tensile stress on the osteoblast differentiation. Tensile stress upregulates the expression of COL I and MMP-1 vial mechano-signal transduction pathways in tension-applied human periodontal ligament cell

II. Research ethics and methods

1. Research ethics

Both MSC and PDLSC were extracted from adipose tissues or periodontal ligament (PDL) tissue around the teeth of human respectively. Cells of passages 2 to 4 were used in the subsequent experiments. The study protocol was approved by the Institutional Review Board of Seoul National University Hospital [C-1401-121-550].

2. Methods

1) Preparation of PDMS Mold

A poly dimethylsiloxane (PDMS) solution was prepared by mixing silicone elastomer base (Sylgard 184, Dow Corning, Midland, MI, USA) and silicone elastomer curing agent (Sylgard 184, Dow Corning) at a ratio of 10:1 (w/w). The prepared PDMS solution was poured onto a master mold and degassed for an hour. After degassing, the PDMS solution was annealed at 80℃ for 4 hr for curing. After curing process, the PDMS mold was peeled off from the master mold. The low surface energy and elasticity of PDMS made itself to be peeled off from the patterned surface easily.

2) Preparation of Pattern on Cell Culture Plate

TPT precursor solution was prepared by mixing TPT (Sigma-Aldrich, St. Louis, MO, USA, Mn=~644) and photo initiator, 2-hydroxy-2-methyl-propiophenone (HOPP) (Sigma-Aldrich, 97%), at a ratio of 95:5 (v/v). The mixed TPT precursor solution was dropped on a cell culture plate and then PDMS mold was placed over it. The TPT precursor solution was cured for 90 min using a wave length 365 ㎚, 135 ㎽/㎠ UV light source (Fusion cure system, Minuta technology, Republic of Korea). After curing process, PDMS mold was peeled off from the patterned TPT. To minimize the residual oligomer of TPT, UV curing process was repeated on patterned TPT for 90 min. Ten types of pattern were used for this study (Table 1). A surface of the patterned structure was modified by ultraviolet ozone (UVO) treatment method using ozone cure system (Minuta technology) for an hour.

3) Measurement of the Contact Angles

The contact angles were measured with Phoenix 150 surface angle analyzer (Surface Electro Optics, Republic of Korea) using deionized water and estimated with an Image XP 5.9. Patterned structure images were took by field-emission scanning electron microscopy (S-4800, Hitachi,Tokyo, Japan).

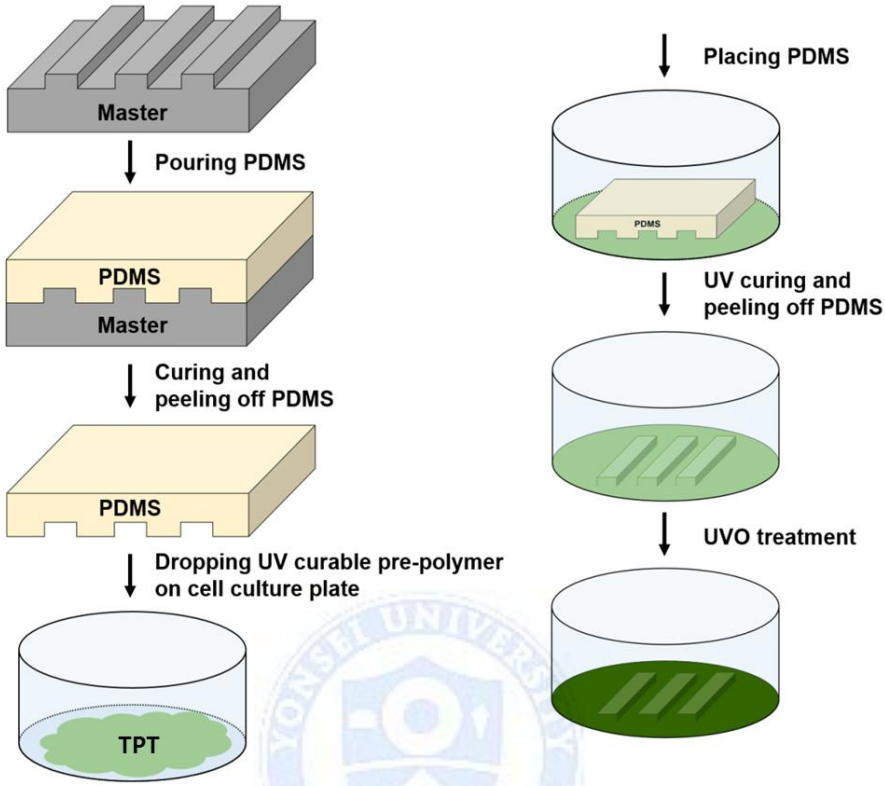

Figure 4. A schematic illustration of the manufacturing procedure of groove patterned TPT.

After pouring PMDS on master pattern, the harden PDMS was cured and peeled off. UV curable pre-polymer was dropped on the cell culture plate, and was placed the PDMS on the plate. UVO and peeling off the PDMS was conducted on the cell culture plate. Finally, UVO was treated to improve the hydrophilicity of groove patterned TPT.

Table 1. Types of groove pattern used in this study

No.	Pattern name	Size		Ridge	Groove
1	Aict-3	Small size pattern		0.35	0.65
2	Aict-2			0.65	0.76
3	Aict-1			0.85	1.10
4	Aict-0			0.43	1.80
5	SU-4	Large size pattern	Groove Fix	2.83	3.00
6	SU-6			5.47	3.00
7	SU-8			7.00	3.00
8	AZ-2		Ridge Fix	2.00	2.00
9	AZ-4			2.00	4.00
10	AZ-6			2.00	6.00

(unit: m)

4) Scanning Electron Microscopy (SEM)

For examining and verifying the topography of the pattern, samples were sputter-coated with a layer of PTP and were imaged with an accelerating voltage of 5 kV using a scanning electron microscope (FE-SEM; S-4800: Hitachi)

5) Atomic Force Microscopy (AFM)

The precision surface topography of the pattern was estimated with an atomic force microscope (AFM; XE150: PSIA, Sungnam, Republic of Korea) in non-contact mode using a Nanoworld AR5-NCHR (Silicon) tip (Neuchâtel, Switzerland). The images were obtained with a scan rate of 0.3 Hz and a sampling resolution of 256 lines • 256 pixels per line.

6) Differentiation of Osteoblast

MC3T3-E1 cells were purchased from American Type Culture Collection (ATCC, Manassas, VA, USA) and maintained in alpha-minimum essential medium (α-MEM) without ascorbic acid supplemented with 10% fetal bovine serum, 1% penicillin/streptomycin, and 1% l-glutamine (All from Life Technologies, Carlsbad, CA, USA).

Adipose tissue was obtained in the course of abdominal local surgery with informed consent. AD-MSC were isolated as previously described [12]. AD-MSCs were maintained in Dulbecco Modified Eagle Medium (DMEM, Life Technologies) mixed with Endothelial Growth Medium (EGM, Lonza, Basel, Switzerland) as conditioned medium (DMEM:EGM = 4:1)

Teeth were obtained in the course of extraction of a tooth in the dentist with informed consent. PDLSC were gently separated from the surface of the root and then digested in a solution of 3 mg/mL collagenase type I (Sigma-Aldrich) and 4 mg/mL dispase (Sigma-Aldrich) for 1 hr at 37℃.

Prior to seeding cells, medium was added into the well of culture plate and incubated for 2 days to make a favorable environment to the cells. Then, cells were seeded with near-confluent density. For the differentiation of osteoblast, both ascorbic acid (100 g/ml, Sigma-Aldrich) and β-glycerophosphate (10 mM, Sigma-Aldrich) were added in culture media. (MC3T3-E1 cells were cultured in α-MEM without ascorbic acid, stem cells were cultured in mixed media combining DMEM and EBM media.)

7) Analysis of Alignment and Morphology of Cells

For determination of alignment and morphology of cultured cells onto groove pattern or nonpattern, cells were seeded onto groove patterns and culture for 2 days prior to imaging. Minimums of 3 randomly selected areas (Olympus microscope, Shinjuku, Tokyo, Japan) in 3 images for each group were analyzed. Analysis was done via computer-assisted morphometry (Rhinoceros 3D, Seattle, WA, USA) or Image J (http://imagej.nih.gov/ij/, National Institute of Health, Bethesda, MD, USA).

8) Mineralization Assay

MC3T3-E1 cells, AD-MSCs, and PDLSC were cultured with appropriate media for differentiation until full differentiation was observed, about 10, 20,

and 8 days, respectively, with changing media every 3 days. At the end of each culture, cells were subjected to Alizarin Red S (Sigma-Aldrich) staining to identify calcium deposits in the cell layer. Briefly, the cells in the well were washed with PBS and fixed in 10% (v/v) formaldehyde at room temperature for 15 min. After washing twice with distilled water, the plate was incubated with 40 nM ARS (pH 4.1) per well for 20 min. Unincorporated dye was washed away with distilled water and aspirated. ImageJ was used for the quantification for calcium deposits in the cell layer.

9) Quantitative RT-PCR

Total RNA was purified from MC3T3-E1 cells cultured in differentiation media with an RNeasy Mini kit (Qiagen, Valencia, CA, USA), according to the manufacturer's protocol. Quantity and purity of RNA was determined by 260/280 nm absorbance (NanoDrop, Wilmington, DE, USA). A cDNA was synthesized from 1 mg of RNA using the cDNA synthesis kit from Roche Applied Science (Indianapolis, IN, USA), as the manufacturer's protocol using a randomized primer. Reverse-transcriptase polymerase chain reaction (RT-PCR) primers are listed in Table 2. Quantitative real-time PCR was performed using the SYBR green PCR master mix from Bioneer (Daejeon, Republic of Korea). Results were analyzed using relative expression calculated using the comparative Ct method and normalized with *GAPDH* expression. To analyze the relative gene expression data, the 2(-Delta Delta C(T)) method was applied [13].

10) Immunohistological Assay

The cells on the pattern fixed with a solution of 4% (v/v) paraformaldehyde after 1 days culture and then permeabilized with a solution of 0.1% Triton X-100 in PBS for 5 min. To reduce non-specific background, sections were treated with 0.2% bovine serum albumin solution in PBS for 20 min. Primary antibodies (Ab) against phospho ERK or phospho NF-κB (p65) (Cell Signaling Technology, Danvers, MA, USA) followed by incubation with HRP-conjugated anti-rabbit Ab (1:1000; Cell Signaling Technology). Chromogenic substrates 3, 3' Diaminobenzidine (DAB) was used to develop. And Mayer's hematoxylin was used as a counterstain for DAB. Image acquisition and processing was performed using a confocal microscope (Olympus).

3. Statistical analysis

Either SPSS software for Windows, version 18.0 (SPSS Inc., Chicago, IL, USA) or Prism version 5 (GraphPad, La Jolla, CA, USA), was used for all statistical analyses. According to results of the Kolmogorov-Smirnov and Sapiro-Wilks tests ($P > 0.05$), nonparametric statistics were used in this study.

Table 2. Primers used in this study

Gene name	Forward primer (5' → 3')	Reverse primer (5' → 3')
Runx2 [14]	CGGCCCTCCCTGAACTCT	TGCCTGCCTGGGATCTGTA
ALPL [14]	TTGTGCCAGAGAAAGAGAGAG	GTTTCAGGCATTTTTCAAG
SP7 [15]	CCCTTCTCAAGCACCAATGG	AGGGTGGGTAGTCATTTGCATAG
BGLAP [14]	CTGACAAAGCCTTCATGTCCAA	GCGGGCGAGTCTGTTCACTA
PIAS [15]	CCTTATTCCAGTTGATCCCCAGT	TATGACCCCTGTCTCACTCCT
GAPDH	CAAGGTCATCCATGACAACTTTG	GGCCATCCACAGTCTTCTGG

III. Results

1. Groove pattern was fabricated from PDMS mold

To make a groove pattern with the polymer, TPT, PDMS mold placed on the surface of the substrate (Figure 4). Groove patterns used in this study (Table 1) can be divided into two groups; 6 types of pattern were large group (Figure 5) and 4 types of pattern were small group (Figure 6). Patterned or nonpatterned TPT structures subsequently were cured by exposure to UVO for several minutes to improve the wettability (Figure 7A).

To test for the changes in the hydrophobicity (wettability) of the patterned TPT surfaces, contact angle (CA) of water on a polystyrene (PS), a bare TPT surface, and a curing TPT was measured. The CA was 45°on the PS, however the CA was 70° on the bare TPT (Figure 7B, left panel). After UVO treatment, the CA of TPT was similar with PS, which is general polymer for cell culture dish. Because the adjusted CA of the water was maintained on the UVO treatment TPT for days, UVO treated TPT was used for this study (Figure 7B, right panel).

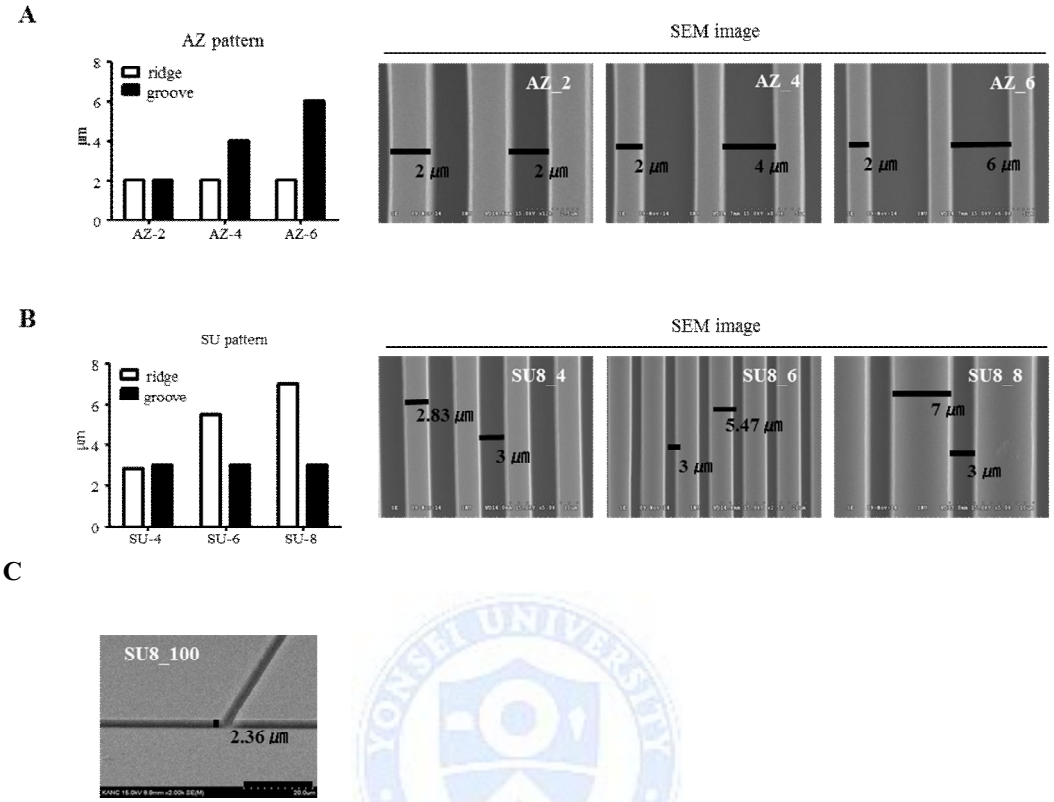

Figure 5. The image of groove patterns in large group

(A) Graph presents comparison of AZ type pattern (left) Representative image of "top-view" SEM each pattern (right) (B) Graph presents comparison of SU type pattern (left) Representative image of "top-view" SEM each pattern (right) (C) Representative image of "perspective view" SEM at the pattern (SU8)

(A)

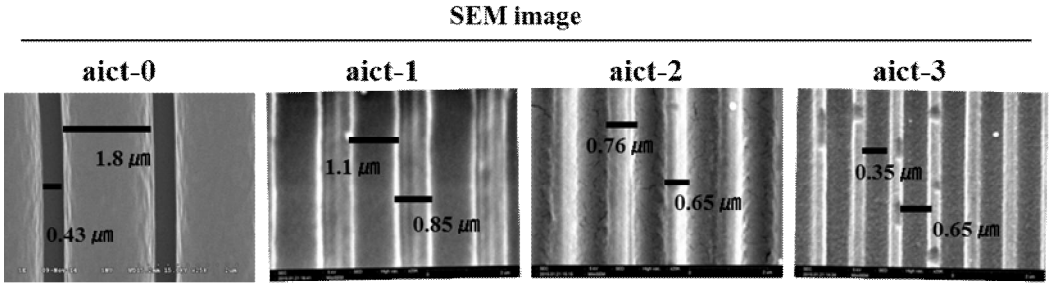

(B)

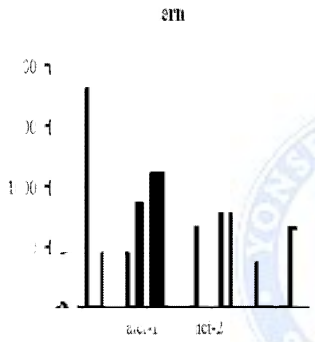

Figure 6. The image of groove patterns in small group

(A) Representative image of “top-view” SEM each pattern (B) Graph presents comparison of aict pattern

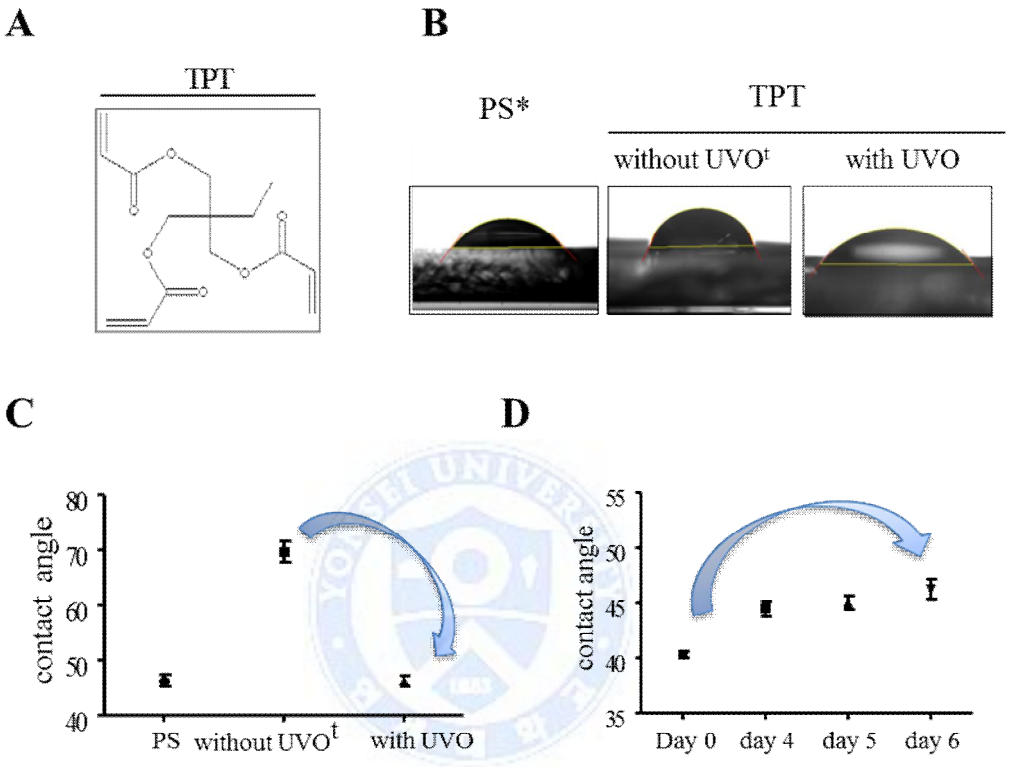

Figure 7. Contact angle of water on surfaces of PS, nonpatterned TPT, and groove patterned TPT by UVO treatment. The contact angle of waster was decreased and it was sustained for a week.

(A) Structural formula of TPT (B) Representative image of contact angle of water on surfaces of PS, patterned TPT without UVO, and patterned TPT with UVO (right) (C) contact angle of water was decreased on the patterned TPT after UVO treatment (D) The contact angle of water was sustained for a week (right)

2. Cells were aligned with linear spindle-shape on groove pattern

On the PS, MC3T3-E1, Ad-MSC, and PDLSC grown with lunate form and the irregular direction. The morphology on the nonpatterned TPT was similar with that on the PS. But, cells attached on the groove patterned TPT have linear spindle-shape with the direction of pattern (Figure 8).

3. Optimal pattern for the differentiation of osteoblast

To compare the extent of osteoblastic differentiation depending on type of pattern, mineralization assay was conducted using Alizarin Red S staining after cultivating cells in the presence of both ascorbic acid (vitamin C) and β-glycerolphosphate on the groove patterned TPT as well as on the nonpatterned TPT. Interestingly, the day of differentiation on the TPT was faster than that on the PS (MC3T3-E1 for 10 days vs. 14 days, Ad-MSC for 20 days *vs*. 30 days, PDLSC for 8 days *vs*. 14 days on PS, respectively). And, the differentiation of osteoblast was enhanced on the groove patterned TPT (at the aict-0, AZ-2, AZ-4) compared to the nonpatterned TPT (Figure 9-10). At the groove pattern, aict-0 was the best to enhance the differentiation of MC3T3-E1. Therefore, the aict-0 type of pattern was selected and used for investigating the mechanism.

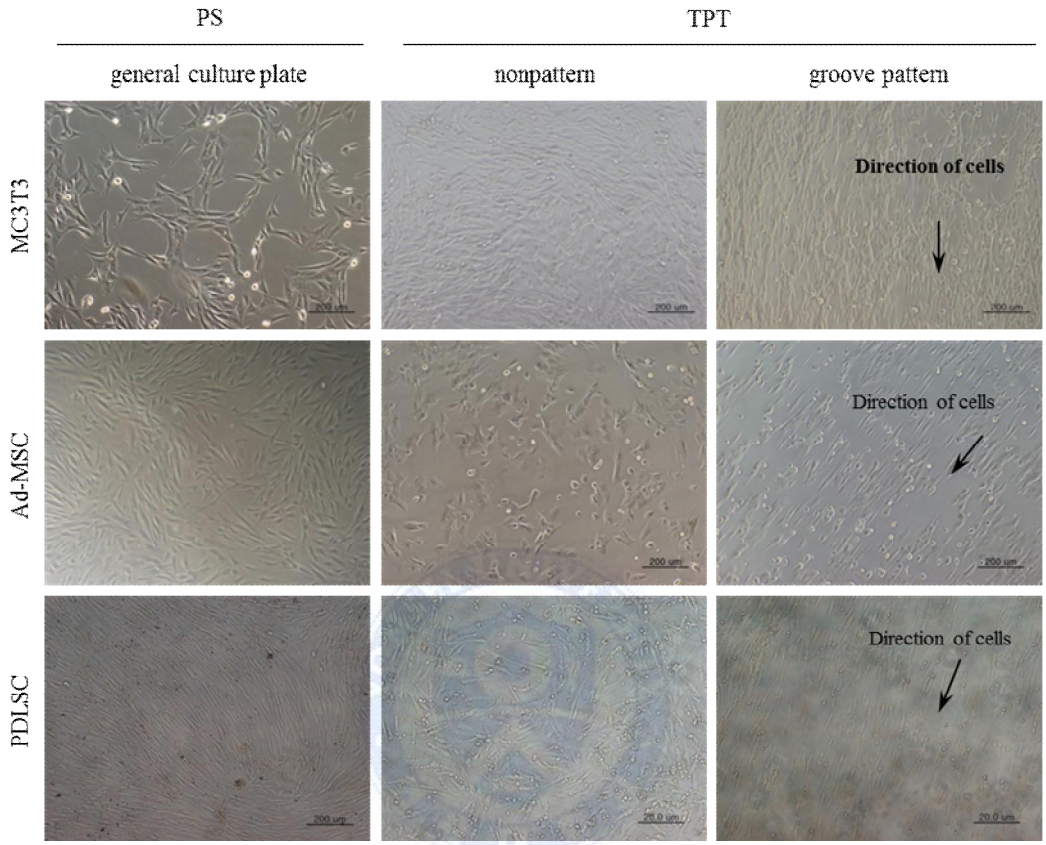

Figure 8. Morphology and orientation of cells were aligned on the patterned TPT

On the PS known a general culture plate, MC3T3-E1, Ad-MSC, and PDLSC attached like a crescent shape (left, middle). However, all cells on the patterned TPT aligned with the direction of pattern (right). Bar = 200 m

A

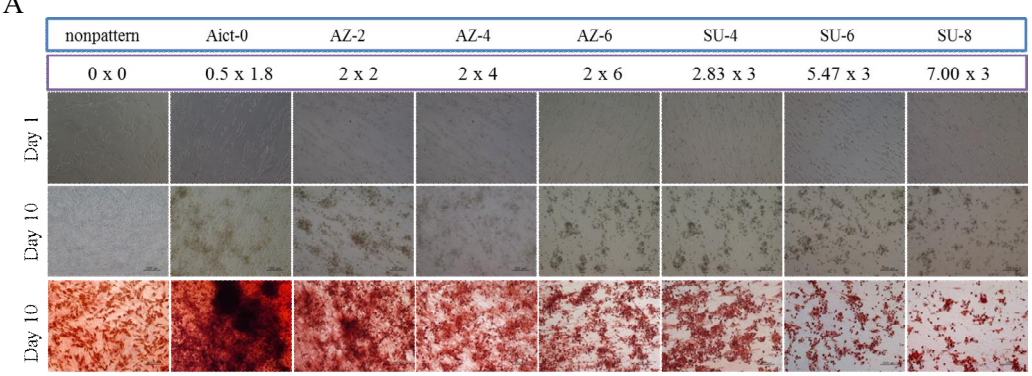

B

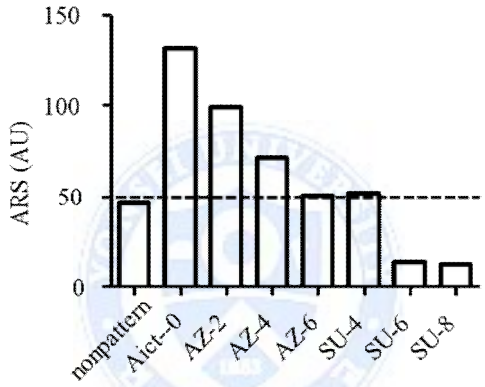

Figure 9. Optimal differentiation of MC3T3-E1 on the groove patterned TPT in large group.

Morphology, orientation, and mineralization of MC3T3-E1 was evaluated on the groove patterned TPT. (A) MC3T3-E1 aligned with the pattern on day 1 after seeding. And mineralization was different depending on the size of pattern in terms of ridge and groove on day 10. (B) Alizarin Red S staining analysis of mineralization was quantified using imageJ. All quantification was normalized by its area. Bar = 200 m

A

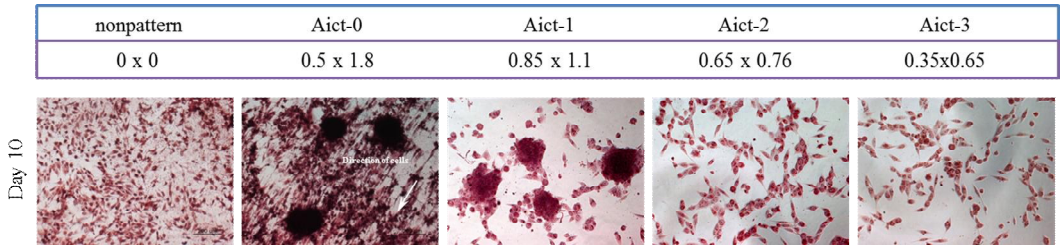

B

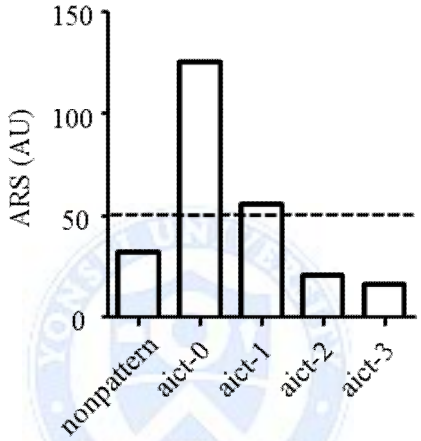

Figure 10. Optimal differentiation of MC3T3-E1 on the groove patterned TPT in small group.

Morphology, orientation, and mineralization of MC3T3-E1 was evaluated on the groove patterned TPT. (A) Mineralization was different depending on the size of pattern in terms of ridge and groove. (B) Alizarin Red S staining analysis of mineralization was quantified using imageJ. All quantification was normalized by its area. Bar = 200 m

4. The kinetics of osteoblastic differentiation was faster on the groove pattern than nonpattern

To determine how fast osteoblastic differentiation occurs, differentiation of pre-osteoblast MC3T3-E1 cells into osteoblast was observed every day. As a result, osteoblastic differentiation was enhanced on the groove patterned TPT compared to the nonpatterned TPT based on calcium deposits (Figure 12). And mineralization was improved on the groove patterned TPT by Alizarin Red S staining (Figure 13, left panel). Differentiation of Ad-MSC as well as PDLSC was superior on the groove patterned TPT than on nonpatterned TPT (Figure 14, Figure 16). Mineralization of Ad-MSC and PDLSC was also enhanced on the groove patterned TPT (Figure 15, Figure 17, left panel).

5. Osteoblastic differentiation was increased on groove pattern despite a half dose osteogenic factor

To further investigate the osteoblastic differentiation on the groove pattern, pre-osteoblasts including MC3T3-E1, Ad-MSC, and PDLSC were differentiated into osteoblast in the condition of a half dose of osteogenic factors, ascorbic acid and β-glycerophosphate (Figure 13, Figure 15, Figure 17). As results, all of pre-osteoblasts were differentiated into osteoblast with calcium deposits, suggesting the groove pattern could reduce the requirement of essential osteogenic factors acting as like osteogenic factor.

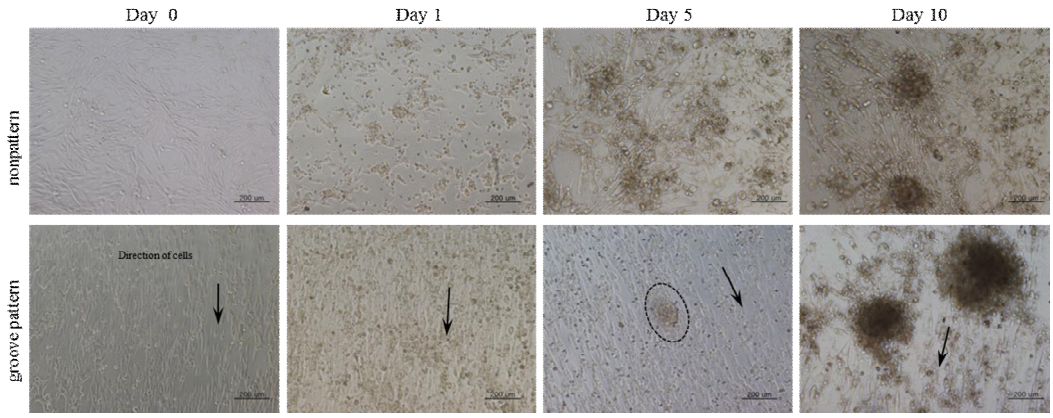

Figure 11. Groove pattern enhanced MC3T3-E1 differentiation. The representative images of MC3T3-E1 were taken on day 0, day 1, day 5, and day 10. Calcium deposit was increased on the groove patterned TPT compared to the nonpatterned TPT. Bar = 200 m

A

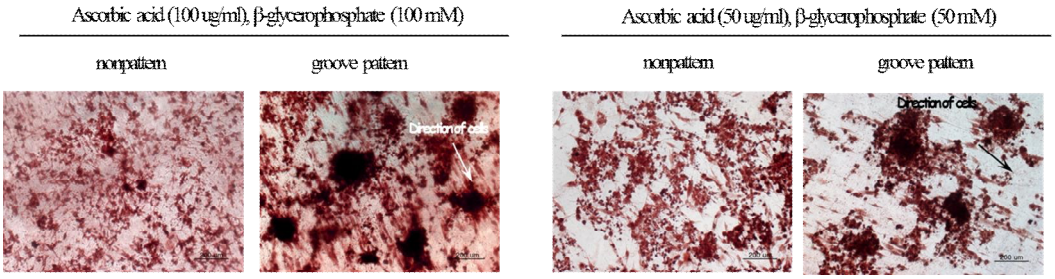

B

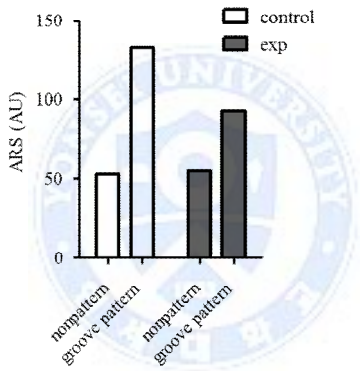

Figure 12. Differentiation of MC3T3-E1 into osteoblast was enhanced after treating a half dose of ascorbic acid

(A) Alizarin Red S staining on day 8 after differentiation. Mineralization was increased on the groove pattern compared to the nonpattern even though the osteogenic factor was halved during differentiation. (B) Alizarin Red S staining analysis of mineralization was quantified using imageJ. All quantification was normalized by its area. Bar = 200 m

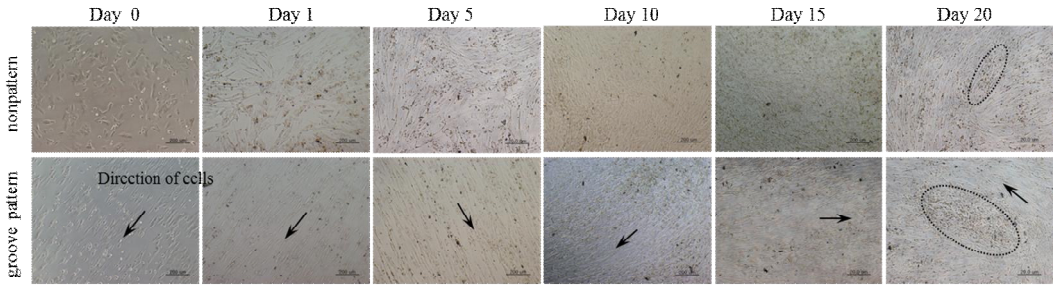

Figure 13. Kinetics of human Ad-MSC differentiation was faster on the groove pattern

The representative images of human Ad-MSC cells were taken on day 0, day 1, day 5, day 10, day 15 and day 20. Calcium deposit was increased on the groove patterned TPT compared to the nonpatterned TPT. Bar = 200 m

A

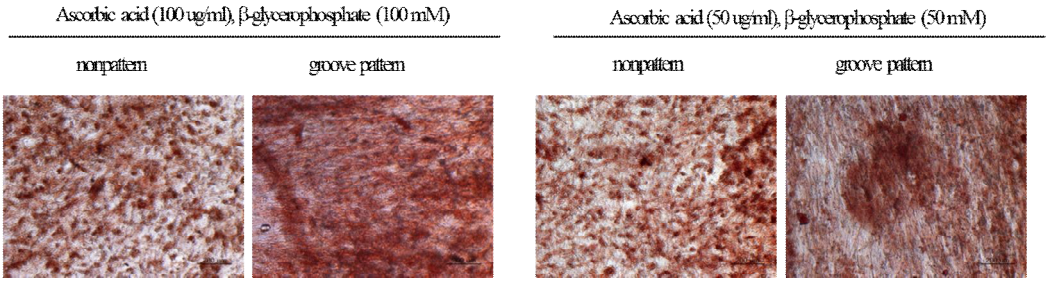

B

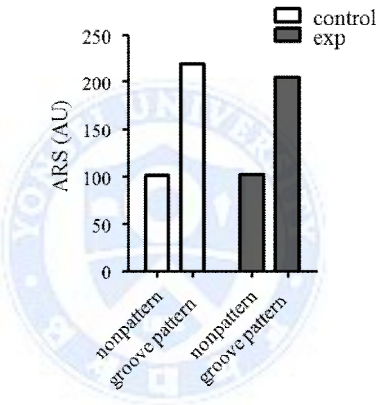

Figure 14. Differentiation of Ad-MSC into osteoblast was enhanced after treating a half dose of ascorbic acid.

(A) Alizarin Red S staining on day 20 after differentiation. Mineralization was increased on the groove pattern compared to the nonpattern (control group) even though the osteogenic factor was halved during differentiation. (B) Alizarin Red S staining analysis of mineralization was quantified using imageJ. All quantification was normalized by its area. Bar = 200 m

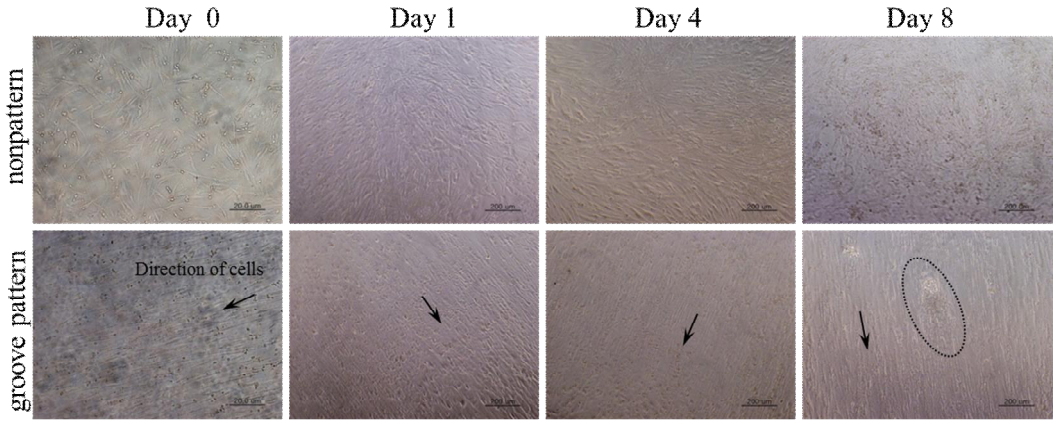

Figure 15. Kinetics of human PDLSC differentiation was faster on the groove pattern

The representative images of human PDLSC cells were taken on day 0, day 1, day 4, and day 8. Calcium deposit was increased on the groove patterned TPT compared to the nonpatterned TPT. All quantification was normalized by its area. Bar = 200 m

A

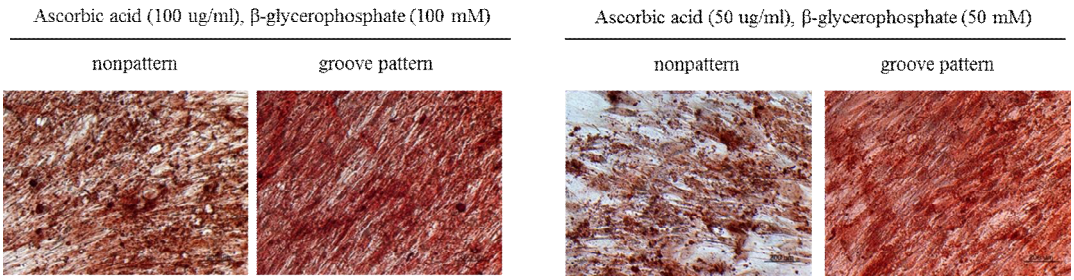

B

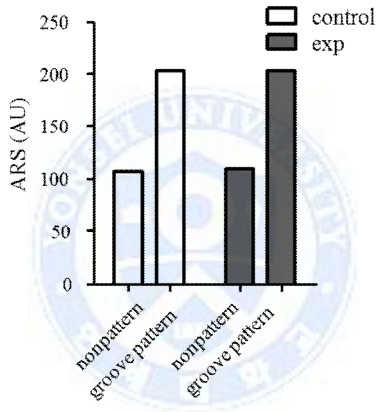

Figure 16. Differentiation of human PDLSC into osteoblast was enhanced after treating a half dose of ascorbic acid.

(A) Alizarin Red S staining on day 8 after differentiation. Mineralization was increased on the groove pattern compared to the nonpattern (control group) even though the osteogenic factor was halved during differentiation. (B) Alizarin Red S staining analysis of mineralization was quantified using imageJ. All quantification was normalized by its area. Bar = 200 m

6. Cell density was important for osteoblastic differentiation

The initial seeding density is a critical variable in functional tissue engineering. Increased seeding density has been shown to result in more aligned and elongated cell nuclei, higher final cell number per construct, and elevated ECM deposition rates compared to lower seeding density [16, 17].

To evaluate whether the cell density dedicate the differentiation of osteoblast, the initial seeding-density was reduced with an eighth sequentially on the PS. As a result, the degree of differentiation was decreased depending on the initial seeding density. These data suggest that cell-cell contact or altered morphology in crowded condition may be important in osteoblastic differentiation (Figure 18).

To exam whether the groove pattern overcome the number of cells during differentiation, cells were grown with one tenth on the groove patterned TPT. After fully differentiation, mineralization was evaluated by Alizarin Red S staining. As a result, calcium deposit was increased on the groove pattern even when the cell number was decreased with one tenth (Figure 19). These data suggest that groove pattern may mimic crowded condition, which is critical condition *in vitro* for osteoblastic differentiation.

A

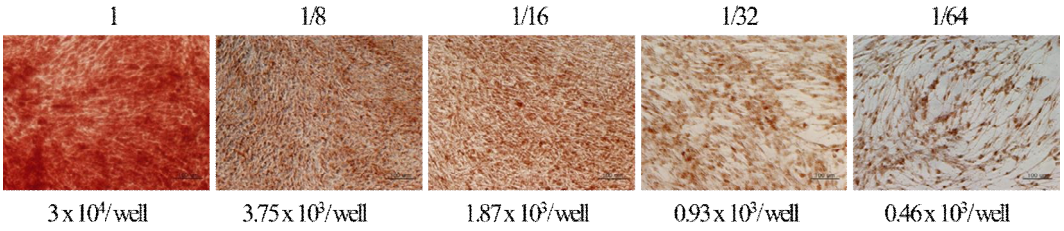

B.

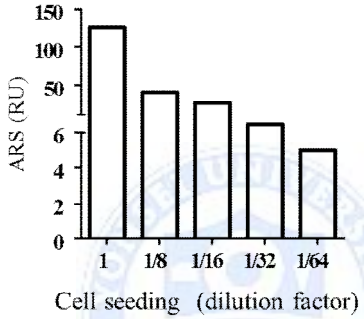

Figure 17. Differentiation of MC3T3-E1 cells into osteoblast was decreased depending on the seeding density on the PS.

(A) The representative images of Alizarin Red S staining on day 14 after differentiation. (B) Alizarin Red S staining analysis of mineralization was quantified using imageJ. All quantification was normalized by its area.

A

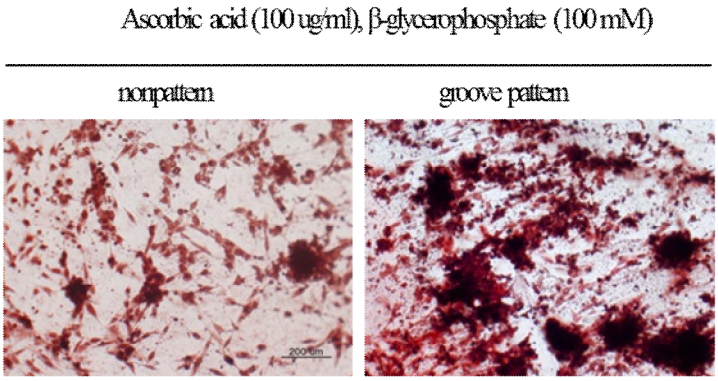

B

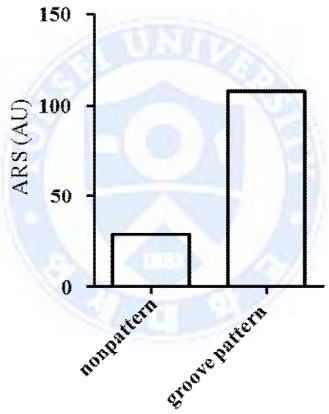

Figure 18. Differentiation of MC3T3-E1 into osteoblast was enhanced despite reducing initial seeding number on the groove patterned TPT

(A) The representative images of Alizarin Red S staining on day 8 after differentiation

Initial seeding number was reduced a tenth of thirty thousand. (B) Alizarin Red S staining analysis of mineralization was quantified using imageJ. All quantification was normalized by its area.

7. Osteoblast differentiation-related gene expression was increased on the groove pattern

Since osteoblastic differentiation was enhanced on the groove patterned TPT, several osteoblastic differentiation-related genes were measured by quantitative RT-PCR. Five genes were used for this study; *RUNX2* (Runt-Related Transcription Factor 2), *Osterix* (Sp7 Transcription Factor), *Osteocalcin* (BGLAP), *ALP* (alkaline phosphatase), *PIASxβ* (Protein Inhibitor of Activated STAT, 2). As results, the expression of *RUNX2* was up-regulated on the groove patterned TPT at the initial stage and down-regulated at the end of differentiation. The expression of *ALP* was more increased on the groove patterned TPT at all stage. The expression of Osterixa and, *PIASxβ* was increased on the groove patterned TPT from the middle of stage; however, the expression of osteocalcin makes no difference between on the groove patterned and on the nonpatterned TPT (Figure19).

A.

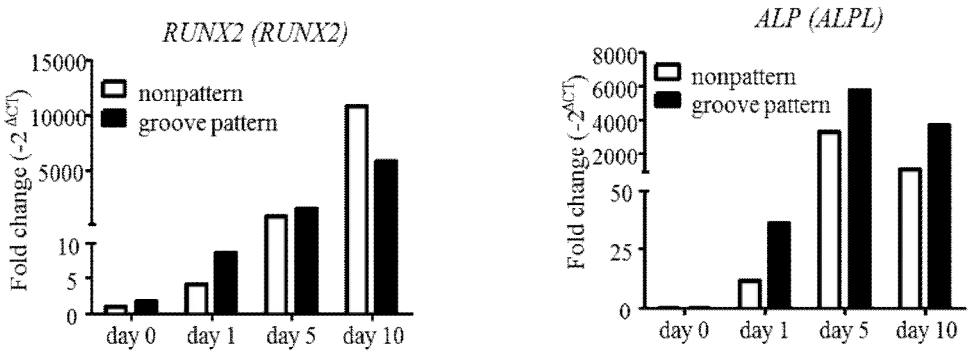

B.

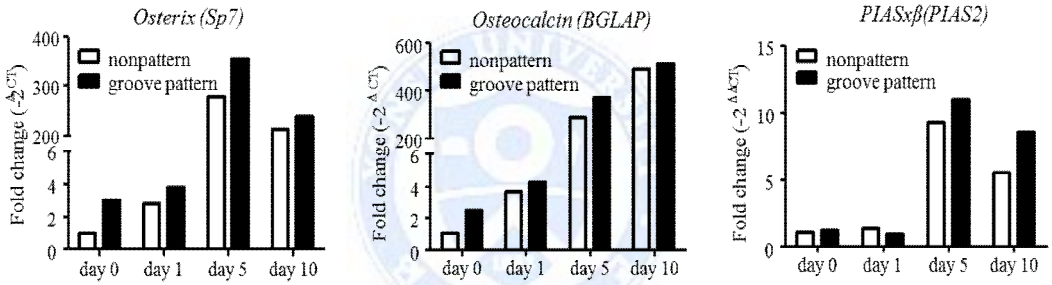

Figure 19. Osteoblastic differentiation markers were increased on the groove pattern.

During differentiation of MC3T3-E1 cells, cells were collected on day 0, day 1, day 5, and day 10 to evaluate the expression of osteoblastic differentiation markers. To analyze the relative gene expression data, the 2(-Delta Delta C(T)) method was applied.

8. Linear morphological change on the groove pattern

Given that cells on the groove pattern TPT were aligned along with the direction of topographical pattern (Figure 8), this morphological change was evaluated by image acquisition of cells on groove patterned and nonpatterned TPT. The shape of cells not only make cells straighten “θ” angle of 15 degree on the groove patterned TPT but also make cells elongate on the patterned TPT compared to the nonpatterned TPT. These deformations in continuum mechanics called strain evoke a tensile stress in the cells on the groove patterned TPT (Figure 20).

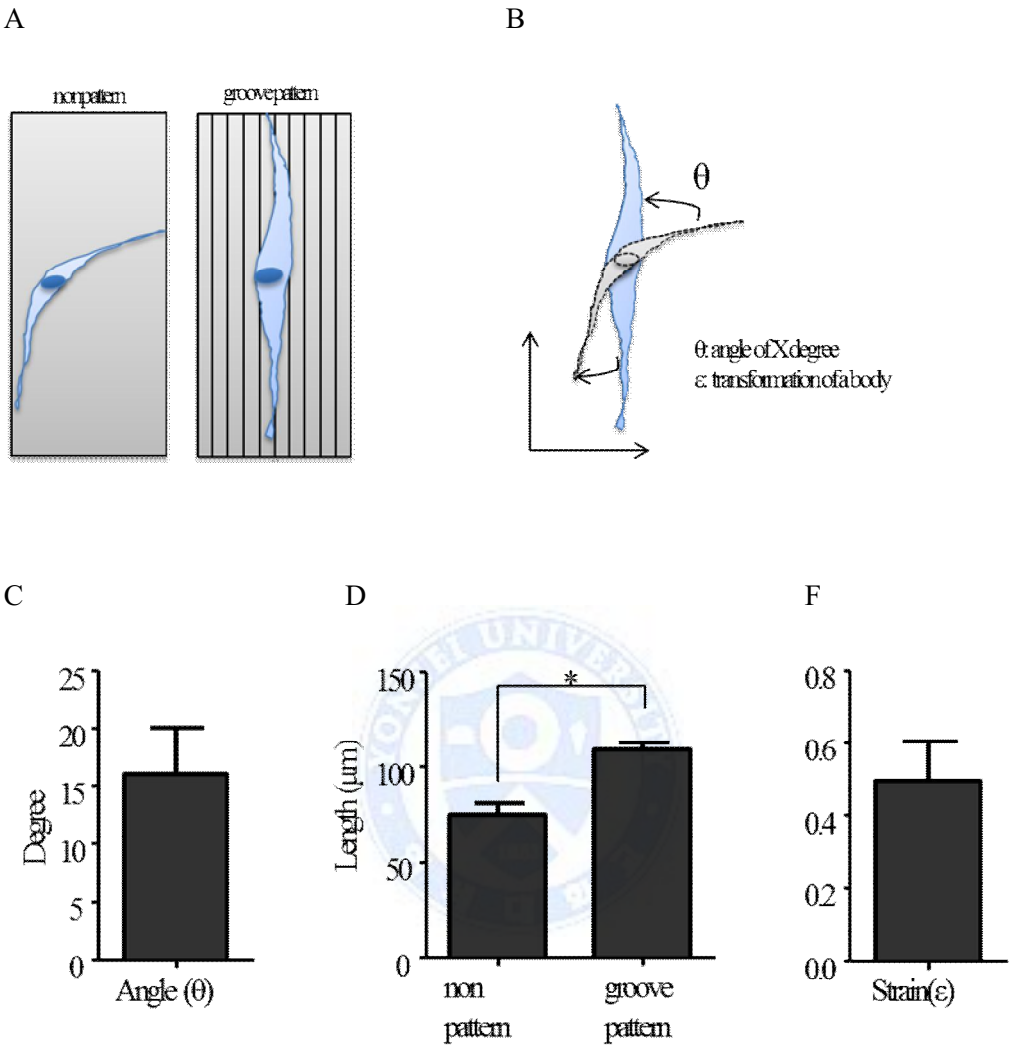

Figure 20. The morphology change of by groove patterned TPT

(A) Illustration of osteoblast on the nonpatterned (left) and on the groove patterned (right) TPT (B-C) angel of degree due to tensile stress (D) elongation of cells (E) extent of transformation of the body

9. Phosphorylation of ERK and NF-κB was increased relatively on the groove pattern

Mechanical loading is considered essential for maintaining skeletal integrity and bone mass. The application of mechanical loading to osteoblasts induces the activation of ERK [18]. To exam whether tensile stress as mechanical loading evoke the activation of ERK in the cells on the groove patterned TPT, phospho-form of ERK was stained by immunohistochemistry (IHC). As a result, phosphorylation of ERK was enhanced on the groove patterned TPT compared to the nonpatterned TPT. Given that ERK can act as an upstream effector of NF-κB signaling in tension-stimulated collagen type 1 [9] (Figure 21A, B), the phosphorylation of NF-κB was analyzed. As a result, phosphorylation of pNF-κB was also improved on the groove patterned TPT compared to the nonpatterned TPT (Figure 21A, B)

When the phosphorylation of both ERK and NF-κB was quantified, expression of both molecules was similar on the nonpatterned TPT and on the groove patterned TPT. However, the expression of pERK was higher than the expression of pp65 on the groove pattern (Figure 21C). Interestingly, the expression of pERK was found in the nucleus on the groove pattern compared to the nonpattern, indicating that pERK could work as a transcriptional factor of genes such as collagen on the groove pattern (Figure 21D).

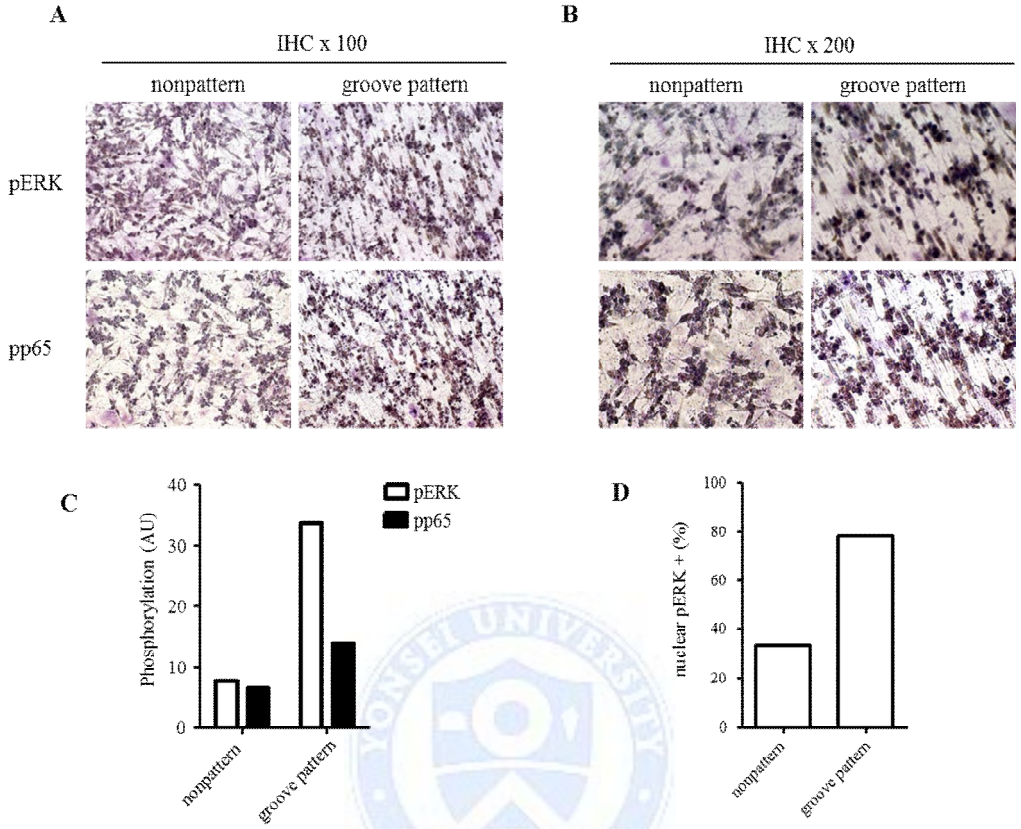

Figure 21. Phosphorylation of ERK, not pp65 on the groove patterned TPT was enhanced relatively on the groove pattern.

After seeding the MC3T3-E1 cells, phosphorylation of both ERK and pNF-κB (pp65) was evaluated by IHC method. ERK phosphorylation was increased in the cells on the groove patterned compared to the nonpatterned TPT. All quantification was normalized by its area. Magnification x 100 (A), x 200 (B). Quantification of phosphorylation both NF-κB (p65) and ERK (C). Quantification of nuclear pERK (D).

10. Gene expression of collagen type 1 was induced on the groove pattern

Vitamin C is a cofactor required for the function of several hydroxylases and monooxygenases, which is an essential step of collagen synthesis at the level of post-transcription. And, there had been reported that the mRNA of collagen type I and type III could be increased to a similar extent by ascorbic acid [19]. To exam whether the groove pattern could induce the gene expression of collagen type 1 without ascorbic acid or whether the groove pattern has synergistic effect with ascorbic acid on the differentiation on the groove pattern, MC3T3-E1 cells were seeded on both nonpatterned and the groove patterned TPT. As a result, the groove pattern induced the expression of *col1a1* weakly on day 3. However, there was no synergistic effect between ascorbic acid and the groove pattern on day 3 (Figure 22).

A

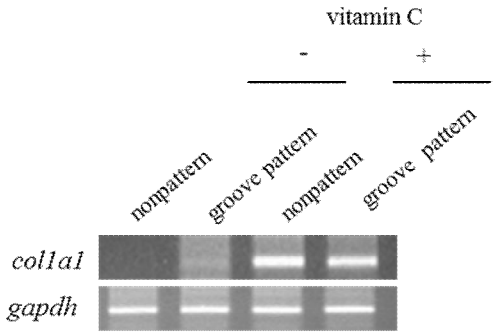

B

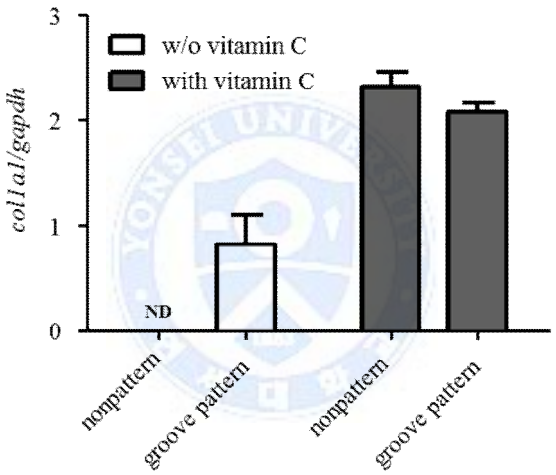

Figure 22. The expression of collagen type 1 gene was increased on the groove patterned TPT

(A) On day 3, transcriptional expression of col1a1 of MC3T3-E1 was measured by RT-PCR on the un-pattern and on the groove pattern. (B) The result was quantified using imageJ. Two independent experiments were conducted. All quantification was normalized by its area.

IV. Discussion

The cells that adhere to the ECM might sense and respond to a wide variety of chemical as well as physical features of the adhesive surface including surface topography [20, 21]. It has been demonstrated that biomaterial surface topography that models features encountered in the native basement membrane can profoundly affect various cell behaviors such as morphology [22-24], cell–substratum adhesion [25, 26], migration [27, 28], proliferation [29, 30], and differentiation [31-33].

Recent experimental studies have shown that the proper tensile strain could have a great effect on the periosteum, leading to osteogenesis as well as micro-environmental changes at the cellular level [34, 35]. Clinically, surface topography of an implant can be designed by making porous and/or by coating the implant surface with other suitable materials to increase osteointegration between bone and implant. Several studies have reported surface modifications of tissue engineering. Therefore I hypothesized that surface topography could affect osteoblast differentiation by tensile stress.

Here, in order to investigate the optimal topographical patterns as a tool to modulate osteoblast differentiation for osseointegration, several nano- or micro-pattern were prepared using TPT polymer. Three types of cell were used to evaluate the differentiation; MC3T3-E1, Ad-MSC, and PDLSC that are possibly differentiated into osteoblast. The differentiation of osteoblast was

enhanced on the groove patterned TPT, which is line and space alignment, compared to nonpatterned TPT even when the osteogenic factor was decreased about a half dose or even when the initial number of seeding cells was reduced about one tenth.

Osteoblastic differentiation-related genes were modulated on the groove patterned TPT compared to the nonpatterned TPT, toward to enhance the differentiation of osteoblast.

Runx2 has been shown to be an essential transcription factor for osteoblast differentiation. Runx2 protein is first detected in preosteoblasts, and the expression is upregulated in immature osteoblasts, but downregulated in mature osteoblasts. In this study, the expression of *Runx2* on the groove patterned TPT was increased in early stage and was decreased in late stage compared with nonpatterned TPT. The expression of *ALP* on the groove patterned TPT, which is a marker of fully differentiation of osteoblast, was increased in late stage, indicating that the pattern on the surface enhances the differentiation of osteoblast compared to nonpatterned TPT. Both *osterix* and *PIASxβ* were expressed highly on the groove patterned TPT in the late stage of differentiation compared to the nonpatterned TPT. However, the expression of *osteocalcin* was similar between on the pattern and on the nonpattern in all stage of differentiation, suggesting that the expression of *osteocalcin* was unaffected by the pattern.

Osteoblasts have important mechanical receptors that can transform

mechanical stress into biochemical signals for bone matrix formation and promote mineralization [36]. Mechanical stress also increases the expression of ECM-related proteins of osteoblasts, including osteonectin, osteopontin (OPN), osteocalcin (OCN), bone morphogenetic protein 2 (BMP-2), and type I collagen [37].

The cells grown on the groove patterned TPT receive mechanical stress. During align following the pattern; the cells suffer from tensile stress. Recently, tensile stress acting on the periosteum that causes tenting of the subperiosteal capsule is sufficient to produce bone formation without a corticotomy [34, 35]. The tension stress might induce differentiation of osteogenic progenitor cells into osteoblasts [38, 39]. In this study, the expression of Runx 2 was increased on the groove patterned TPT compared to the nonpatterned TPT, indicating that tensile stress might up-regulating osteogenic factor expression as previously shown [40].

This study reports meaningful results for topographical pattern to modulate the differentiation of osteoblast by upregulating of osteoblastic differentiation gene in early stage due to tensile stress. However, the results of this study have limitations, such as a restricted pattern with in vitro experiment only. Therefore additional studies are necessary to evaluate other kinds of pattern to enhance the differentiation of osteoblast and to apply for clinical application of pattern.

VI. References

1. Branemark, P.I., *Vital microscopy of bone marrow in rabbit.* Scand J Clin Lab Invest, 1959. **11 Supp 38**: p. 1-82.

2. Bettinger, C.J., Langer, R., and Borenstein, J., *Engineering substrate topography at the micro- and nanoscale to control cell function.* Angew Chem Int Ed Engl 2009. **48**: p. 5406.

3. Brindha, M., N.K. Kumaran, and K. Rajasigamani, *Evaluation of tensile strength and surface topography of orthodontic wires after infection control procedures: An in vitro study.* J Pharm Bioallied Sci, 2014. **6**(Suppl 1): p. S44-8.

4. Dalby, M.J., et al., *The control of human mesenchymal cell differentiation using nanoscale symmetry and disorder.* Nat Mater, 2007. **6**(12): p. 997-1003.

5. Guilak, F., et al., *Control of stem cell fate by physical interactions with the extracellular matrix.* Cell Stem Cell, 2009. **5**(1): p. 17-26.

6. Robling, A.G., A.B. Castillo, and C.H. Turner, *Biomechanical and molecular*

regulation of bone remodeling. Annu Rev Biomed Eng, 2006. **8**: p. 455-98.

7. Butcher, D.T., T. Alliston, and V.M. Weaver, *A tense situation: forcing tumour progression.* Nat Rev Cancer, 2009. **9**(2): p. 108-22.

8. Ikegame, M., et al., *Tensile stress induces bone morphogenetic protein 4 in preosteoblastic and fibroblastic cells, which later differentiate into osteoblasts leading to osteogenesis in the mouse calvariae in organ culture.* J Bone Miner Res, 2001. **16**(1): p. 24-32.

9. Kook, S.H., Y.S. Jang, and J.C. Lee, *Involvement of JNK-AP-1 and ERK-NF-kappaB signaling in tension-stimulated expression of type I collagen and MMP-1 in human periodontal ligament fibroblasts.* J Appl Physiol (1985), 2011. **111**(6): p. 1575-83.

10. Jeon, Y.M., et al., *Role of MAPK in mechanical force-induced up-regulation of type I collagen and osteopontin in human gingival fibroblasts.* Mol Cell Biochem, 2009. **320**(1-2): p. 45-52.

11. Kook, S.H., et al., *Mechanical force induces type I collagen expression in human periodontal ligament fibroblasts through activation of ERK/JNK and AP-1.* J Cell Biochem, 2009. **106**(6): p. 1060-7.

12. Kim, J.H., et al., *Paradoxical effects of human adipose tissue-derived*

mesenchymal stem cells on progression of experimental arthritis in SKG mice. Cell Immunol, 2014. **292**(1-2): p. 94-101.

13. Livak, K.J. and T.D. Schmittgen, *Analysis of relative gene expression data using real-time quantitative PCR and the 2(-Delta Delta C(T)) Method.* Methods, 2001. **25**(4): p. 402-8.

14. Hassan, M.Q., et al., *BMP2 commitment to the osteogenic lineage involves activation of Runx2 by DLX3 and a homeodomain transcriptional network.* J Biol Chem, 2006. **281**(52): p. 40515-26.

15. Ali, M.M., et al., *PIASxbeta is a key regulator of osterix transcriptional activity and matrix mineralization in osteoblasts.* J Cell Sci, 2007. **120**(Pt 15): p. 2565-73.

16. Martin, I., D. Wendt, and M. Heberer, *The role of bioreactors in tissue engineering.* Trends Biotechnol, 2004. **22**(2): p. 80-6.

17. Awad, H.A., et al., *In vitro characterization of mesenchymal stem cell-seeded collagen scaffolds for tendon repair: effects of initial seeding density on contraction kinetics.* J Biomed Mater Res, 2000. **51**(2): p. 233-40.

18. Lee, D.Y., et al., *Integrin-mediated expression of bone formation-related*

genes in osteoblast-like cells in response to fluid shear stress: roles of extracellular matrix, Shc, and mitogen-activated protein kinase. J Bone Miner Res, 2008. **23**(7): p. 1140-9.

19. Nusgens, B.V., et al., *Topically applied vitamin C enhances the mRNA level of collagens I and III, their processing enzymes and tissue inhibitor of matrix metalloproteinase 1 in the human dermis.* J Invest Dermatol, 2001. **116**(6): p. 853-9.

20. Li, D., et al., *Role of mechanical factors in fate decisions of stem cells.* Regen Med, 2011. **6**(2): p. 229-40.

21. Schvartzman, M., et al., *Nanolithographic control of the spatial organization of cellular adhesion receptors at the single-molecule level.* Nano Lett, 2011. **11**(3): p. 1306-12.

22. Teixeira, A.I., et al., *Epithelial contact guidance on well-defined micro- and nanostructured substrates.* J Cell Sci, 2003. **116**(Pt 10): p. 1881-92.

23. Crouch, A.S., et al., *Correlation of anisotropic cell behaviors with topographic aspect ratio.* Biomaterials, 2009. **30**(8): p. 1560-7.

24. Huang, N.F., et al., *Myotube assembly on nanofibrous and micropatterned polymers.* Nano Lett, 2006. **6**(3): p. 537-42.

25. Karuri, N.W., et al., *Nano- and microscale holes modulate cell-substrate adhesion, cytoskeletal organization, and -beta1 integrin localization in SV40 human corneal epithelial cells.* IEEE Trans Nanobioscience, 2006. **5**(4): p. 273-80.

26. Karuri, N.W., et al., *Biological length scale topography enhances cell-substratum adhesion of human corneal epithelial cells.* J Cell Sci, 2004. **117**(Pt 15): p. 3153-64.

27. Diehl, K.A., et al., *Nanoscale topography modulates corneal epithelial cell migration.* J Biomed Mater Res A, 2005. **75**(3): p. 603-11.

28. Kaiser, J.P., A. Reinmann, and A. Bruinink, *The effect of topographic characteristics on cell migration velocity.* Biomaterials, 2006. **27**(30): p. 5230-41.

29. Liliensiek, S.J., et al., *The scale of substratum topographic features modulates proliferation of corneal epithelial cells and corneal fibroblasts.* J Biomed Mater Res A, 2006. **79**(1): p. 185-92.

30. Christopherson, G.T., H. Song, and H.Q. Mao, *The influence of fiber diameter of electrospun substrates on neural stem cell differentiation and proliferation.* Biomaterials, 2009. **30**(4): p. 556-64.

31. Dang, J.M. and K.W. Leong, *Myogenic Induction of Aligned Mesenchymal Stem Cell Sheets by Culture on Thermally Responsive Electrospun Nanofibers.* Adv Mater, 2007. **19**(19): p. 2775-2779.

32. Yim, E.K., S.W. Pang, and K.W. Leong, *Synthetic nanostructures inducing differentiation of human mesenchymal stem cells into neuronal lineage.* Exp Cell Res, 2007. **313**(9): p. 1820-9.

33. Oh, S., et al., *Stem cell fate dictated solely by altered nanotube dimension.* Proc Natl Acad Sci U S A, 2009. **106**(7): p. 2130-5.

34. Schmidt, B.L., et al., *Induced osteogenesis by periosteal distraction.* J Oral Maxillofac Surg, 2002. **60**(10): p. 1170-5.

35. Kostopoulos, L. and T. Karring, *Role of periosteum in the formation of jaw bone. An experiment in the rat.* J Clin Periodontol, 1995. **22**(3): p. 247-54.

36. Wozniak, M., et al., *Mechanically strained cells of the osteoblast lineage organize their extracellular matrix through unique sites of alphavbeta3-integrin expression.* J Bone Miner Res, 2000. **15**(9): p. 1731-45.

37. Yoo, H.D., et al., *Impedance analysis for hydrogen adsorption pseudocapacitance and electrochemically active surface area of Pt*

electrode. Langmuir, 2009. **25**(19): p. 11947-54.

38. Shimizu, T., et al., *Osteoblastic differentiation of periosteum-derived cells is promoted by the physical contact with the bone matrix in vivo.* Anat Rec, 2001. **264**(1): p. 72-81.

39. Takushima, A., Y. Kitano, and K. Harii, *Osteogenic potential of cultured periosteal cells in a distracted bone gap in rabbits.* J Surg Res, 1998. **78**(1): p. 68-77.

40. Kanno, T., et al., *Tensile mechanical strain up-regulates Runx2 and osteogenic factor expression in human periosteal cells: implications for distraction osteogenesis.* J Oral Maxillofac Surg, 2005. **63**(4): p. 499-504.

국문요약

나노표면 패턴의 조골세포 분화 효과

<지도교수: 이 기 준, D.D.S., M.S.D., Ph.D.>

연세대학교 대학원 치의학과

김 창 수

세포는 세포외기질의 구조 및 조정에 따라 세포의 모양, 활성화, 분화, 운동, 및 운명을 조절하기 때문에 다양한 동물세포를 이용하여 '표면지형'이 세포에 어떤 영향을 미치는지에 대한 많은 연구가 있다. 세포와 표면지형 사이의 접촉은 첫째 세포가 인지하는 세포외기질의 내의 현상이며, 둘째 세포의 모양, 방향, 행동을 변화하여 세포 내 신호전달계를 변화시킬 수 있다.

한 예로 치아 임플란트의 표면지형은 임플란트 이식의 성공과 장기 예후에 중요한 역할을 한다. 따라서 이식된 임플란트가 좀 더 초기에 안착하고 좀 더 오랫동안 그 기능이 유지되어 뼈에 단단하게 이식될 수 있도록 임상적 연구와 실험적 연구가 계속적으로 이뤄지고 있다. 하지만 아직까지도 조골세포나 파골세포의 분화를 강화시키는 표면지형의 규칙에 대해서는 찾지 못했다. 이는 표면지형을 조성함에 있어서 조골세포의 분화기전에 의해서 디자인하지 않고, 무작위적인 방법으로 형성하였기 때문이다.

따라서 본 연구에서는 조골세포의 분화를 조절하는 표면지형을 디자인하여 제작하고, 이를 트리메틸올프로판 트리아크릴레이트 위에 패턴으로 제작

한 후 생쥐의 조골세포 전구체, 사람의 지방유래 중간엽 줄기세포, 사람의 치주인대 줄기세포를 이용하여 조골세포 정도를 분석하였다. 조골세포의 분화는 미네랄화 정도 및 조골세포와 관련된 유전자 발현으로 분화를 평가하였다.

실험결과, 조골세포의 분화는 패턴이 없을 때보다 특정 규칙의 홈이 존재하는 패턴 위에서 세포를 분화시켰을 때 조골세포의 분화율이 증가하였고, 분화요소를 절반으로 처리하거나 초기 파종한 세포의 수가 줄어도 (십분의 일) 홈이 있는 패턴 위에서 조골세포의 분화가 강화되었다. 이는 특정 규칙의 홈이 있는 패턴이 조골세포의 장력을 유발하기 때문이며, 이러한 장력 스트레스가 얼크의 인산화를 증가시킴으로써 조골세포의 분화 촉진에 도움이 되었을 것으로 사료된다.

본 연구결과는 특정 규칙을 갖은 표면패턴이 장력을 기반으로 조골세포 생성을 조절하는 역할을 할 수 있음을 시사하며, 궁극적으로 조골세포의 분화가 중요한 의료기기 및 재료 개발에 중요한 근거를 제공할 것으로 사료된다.

핵심 단어: 표면패턴, 조골세포 분화, 기계적 스트레스(장력)